# Pattern induced phase transition of vortex motion in high-$T_c$ films

R. Wördenweber, E. Hollmann, J. Schubert, R. Kutzner, and Ajay Kumar Ghosh

Citation: Appl. Phys. Lett. **94**, 202501 (2009);
View online: https://doi.org/10.1063/1.3139077
View Table of Contents: http://aip.scitation.org/toc/apl/94/20
Published by the American Institute of Physics

# Pattern induced phase transition of vortex motion in high-$T_c$ films

R. Wördenweber,[1,a)] E. Hollmann,[1] J. Schubert,[1] R. Kutzner,[1] and Ajay Kumar Ghosh[1,2]
[1]*Institut für Bio-und Nanotechnologie (IBN) and JARA-Fundamentals of Future Information Technology, Forschungszentrum Jülich, D-52425 Jülich, Germany*
[2]*Department of Physics, Jadavpur University, Kolkata 700 032, India*

(Received 24 March 2009; accepted 23 April 2009; published online 18 May 2009)

A micropattern induced transition in the mechanism of vortex motion and vortex mobility is demonstrated for high-$T_c$ films. The competition between the anomalous Hall effect and the guidance of vortices by rows of microholes (antidots) leads to a sudden change in the direction of vortex motion that is accompanied by a change of the critical current density and microwave losses. The latter demonstrates the difference in vortex mobility in the different phases of vortex motion in between and within the rows of antidots. © *2009 American Institute of Physics*.
[DOI: 10.1063/1.3139077]

The dynamics of magnetic flux quanta (vortices) in superconductors share similarities with quanta of electrical charge (electrons) in solids.[1] Exploring ways to control the motion of vortices has turned out to be useful for the understanding of vortex physics, for the improvement of existing superconducting devices and for the development of innovative fluxtronic devices that employ vortices instead of electrons. Superconductors with periodic arrangements of pinning centers have been proven to be ideal systems for studying dynamical phenomena of vortex movement. Starting from the demonstration of commensurability effects in superconducting thin films with regular arrays of submicrometer holes (antidots),[2–6] it has been demonstrated that local vortex trapping and guidance of magnetic flux can be achieved via strategically positioned antidots and antidot arrays.[7,8] Vortex ratchet effects in conventional,[9–11] as well as high-$T_c$ thin films (HTS) (Ref. 8) with periodic structures breaking the symmetry of the vortex pinning potential point the way toward more complex fluxtronic concepts.[12] In all these concepts the manipulation of vortices via patterning is essential.

In this paper we demonstrate that a transition of the vortex motion can be induced by artificial defects in HTS thin films. A special arrangement of arrays of antidots in high-$T_c$ films leads to guided vortex motion that sets in at a clearly defined temperature. The inversion of the longitudinal component of vortex motion and the resulting change of the mobility of vortices is demonstrated via combined dc and microwave measurements.

High-$T_c$ films are prepared on microwave suitable substrates. $YBa_2Cu_3O_7$ (YBCO) is deposited on $CeO_2$ buffered sapphire. A film thickness of $d \approx 50-100$ nm is chosen in order to obtain a large effective penetration length and small critical currents. The latter is important to avoid local heating especially at the contact during flux flow experiments. The zero-temperature effective penetration depth $\lambda_{\text{eff}} = \lambda_L \coth(d/2\lambda_L)$ (Ref. 13) is about $\sim 1.4 - \sim 0.7$ $\mu$m for our 50–100 nm thick YBCO films, respectively. Due to the lattice mismatch, a slight reduction of the transition temperature ($T_c \approx 88-89$ K) is obtained. Arrays of holes (antidots) are generated via optical lithography and ion beam etching. In these experiments pairs of rows of antidots (diameter of $1.2 \pm 0.05$ $\mu$m) are used. The geometrical arrangement of the rows is shown in Fig. 1, the distance between adjacent antidots in the row is $\sim 4.8$ $\mu$m (edge-to-edge). In order to optimize the Hall signal due to guidance, an orientation of the rows with respect to the Lorentz force (perpendicular to the current direction) of $\gamma = \pm 35°$ is chosen. For this angle the largest Hall signal have been obtained in previous measurements of angular dependent guided vortex motion via rows of antidots.[14,15]

Critical properties and vortex dynamic are analyzed via combined resistive and microwave 6-probe measurements. A microwave signal (0.05–20 GHz, up to 5 dBm maximum input power) is added to a dc current that is applied to the superconducting stripline. The longitudinal and transverse (i.e., Hall signal) components of the dc voltage characterize the transverse ($\langle v_y \rangle$) and longitudinal ($\langle v_y \rangle$) components of the motion of vortices, respectively (see Fig. 1). Simulta-

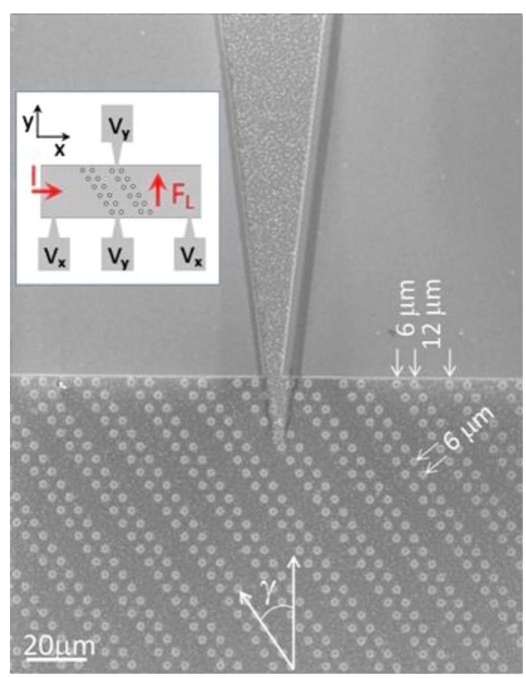


FIG. 1. (Color online) Sketch of the sample design (inset) and image of a section of the sample depicting one of the Hall contacts and the antidot arrangement. The angle $\gamma$ is defined by the nominal direction of the Lorentz force and the orientation of rows of antidots.

[a)]Author to whom correspondence should be addressed. Electronic mail: r.woerdenweber@fz-juelich.de.

 

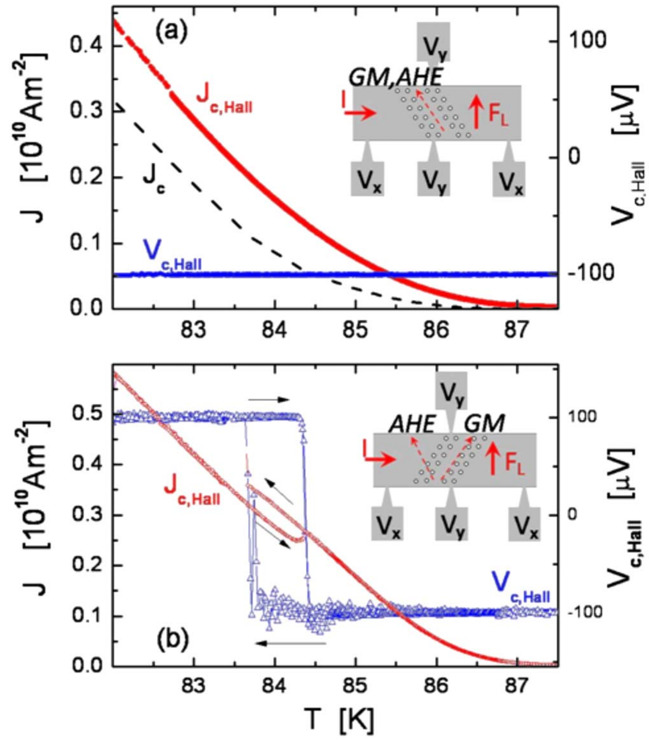


FIG. 2. (Color online) Critical current densities $J_c$ (black dashed line) and $J_{c,\mathrm{Hall}}$ (red symbols) for two different orientations of rows of antidots $\gamma=-35°$ (a) and $\gamma=+35°$. $J_{c,\mathrm{Hall}}$ is defined by a Hall voltage $|V_{c,\mathrm{Hall}}|=100$ $\mu$V (blue triangles). The arrows indicate the direction of temperature change during the experiment, the magnetic field was 0.6 mT. The different designs (i.e., different orientation of the rows of antidots) are sketched in the insets, the directions of the current and the different interactions acting on the vortices are indicated.

neously, the microwave transmission coefficient $S_{21}$ is recorded. The latter provides a measure for the losses due to vortex motion. The different components—longitudinal voltage, Hall signal, and microwave loss—are shown in Figs. 2 and 3 and are discussed in the following.

The longitudinal voltage represents the standard parameter to characterize the critical properties of a superconducting stripline. In the superconducting regime, it is generated by vortex motion along the Lorentz force, i.e., across the stripline. It characterizes the average velocity component $\langle v_y \rangle$ of vortex between the voltage contacts $V_x$ and defines a critical current density $J_c$. For our samples, $J_c$ shows the classical behavior for both arrangements of rows of antidots. It increases monotonously with decreasing temperature [Fig. 2(a)].

In contrast, the Hall signal $V_{\mathrm{Hall}}$, provides a local characterization of the component $\langle v_x \rangle$ of vortex motion, i.e., perpendicular to the Lorentz force $F_L$. It probes the effect of forces acting on vortices others than $F_L$. Figure 2 shows the result of Hall measurements for both orientations of rows of antidots. Similar to measurements of the critical current, we kept the component of vortex motion $\langle v_x \rangle$ constant by controlling the Hall signal, $|V_{c,\mathrm{Hall}}|=100$ $\mu$V. This way, a critical current density $J_{c,\mathrm{Hall}}$ is defined in analogy to $J_c$.

Depending on the orientation of the antidot rows and the magnetic field direction, different temperature dependences are observed.

(i) For the first design [$\gamma=-35°$, Fig. 2(a)] the Hall signal is negative over the whole temperature regime, the vortices move in the direction of the rows [dashed arrow, inset of Fig. 2(a)]. $J_{c,\mathrm{Hall}}$ increases monotonically with decreasing temperature. It agrees qualitatively with the expected behavior of the critical current $J_c$ in the superconducting state (dashed line). The quantitative difference between $J_c$ and $J_{c,\mathrm{Hall}}$ is explained by differences in the voltage criteria that defines different average vortex velocities in different directions.

(ii) In contrast, the second design shows a unique behavior [Fig. 2(b)]. The Hall voltage changes sign in the superconducting regime. A negative voltage is present close to $T_c$, i.e., the vortices do not follow the guidance of antidot rows. At lower temperature the Hall voltage changes abruptly to a positive value, i.e., now the vortices move in the direction of antidot rows. This change of direction of vortex motion is hysteretic, i.e., it occurs at 83.7 and 84.4 K for decreasing and increasing temperatures, respectively. It is accompanied by a hysteretic change of the critical current $J_{c,\mathrm{Hall}}$ [Fig. 2(b)] and a change of the microwave transmission coefficient $S_{21}$ (Fig. 3) at exactly the same temperatures. The modification of the Hall voltage, critical current and microwave properties are indications for a change of the mechanism of vortex motion in the second sample. It is discussed in the following.

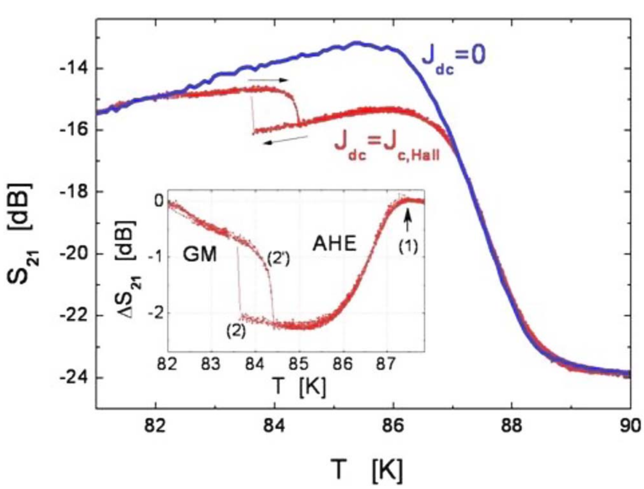


FIG. 3. (Color online) Temperature dependence of the microwave transmission coefficient $S_{21}$ of the design shown in Fig. 2(b) ($\gamma=+35°$) for dc current densities $J=0$ and $J=J_{c,\mathrm{Hall}}$. The inset depicts the difference of $S_{21}$ obtained for both currents. The data are recorded at a frequency of 1 GHz, rf-power of −17 dBm at the sample and a magnetic field of 0.6 mT. The positions 1, 2, and 2′ mark the onset of vortex nucleation and phase transitions of vortex motion, respectively.

Close to $T_c$, a negative Hall voltage is indicative for the presence of the anomalous Hall effect (AHE).[14,16–23] The vortex-pin interaction is weak in this temperature regime. This holds also for the vortex-antidot interaction. As a consequence, the impact of the antidots on vortex motion is weak and, thus, guidance by the rows of antidots is negligible. In this temperature regime the AHE dominates and vortices move in the direction defined by the AHE, as indicated in the insets of Fig. 2. At lower temperature, the vortex-antidot interaction increases and finally, the guidance of vortices via the rows of antidots starts to dominate the

AHE. The vortices move within the rows of antidots.[15]

Depending of the orientation of the rows of antidots, this induces a change of the direction of the component of vortex motion $\langle v_x \rangle$. No change of direction is necessary for the first design [Fig. 2(a)], AHE and guided motion via antidot rows point in the same $x$-direction. Therefore, the Hall voltage stays negative, changes of the critical current density and microwave properties are not observed. In contrast, a change of direction of motion is necessary for a transition from AHE to guided motion for the second design [Fig. 2(b)]. Close to $T_c$ vortices shuttle between the rows of antidots, at lower temperature they move within the rows of antidots. This implies a modification of the mechanism of vortex motion. Whereas vortices mainly travel in the superconductor in the first case, they "hop" from antidot to antidot in the latter case. The difference in the mechanism of vortex motion is visible in the resulting modifications of the critical current density and the microwave loss. The critical current is modified by 10%–12% at the transition. Vortex motion within the rows of antidots seems to be easier than it is in the superconducting matrix. This agrees with results obtained from imaging of vortex motion in microstructured YBCO films.[15] Thus, the guidance of vortices by antidots is based on the reduction of the potential for vortex motion along the row of antidots.

The microwave properties provide indications for the mobility of vortices and the residence time of the vortices in the superconductor. The transition to the superconducting state at $T_c \approx 88.5$ K leads to an increase of $S_{21}$ due to the strong reduction of the microwave surface resistance in the superconducting state (Fig. 3). Below $T_c$, $S_{21}$ is independent of the applied dc current. At lower temperatures ($\sim 87.4$ K) a difference in $S_{21}$ measured for zero current and critical current becomes visible (see inset Fig. 3). This demonstrates that (a) vortices are first formed at this temperature and (b) that the motion of vortices due to the applied current leads to additional microwave losses. The losses increase with decreasing temperature and saturate at a value of $\Delta S_{21} \approx 2.1$ dB. In this temperature regime the AHE dominates the longitudinal vortex motion, vortices shuttle between the rows of antidot, i.e., they mainly move in the superconductor. The losses due to moving vortices are relatively large. At lower temperature, the transition to guided motion via antidot rows takes place. For decreasing temperature, this causes an increase of the transmission coefficient by more than 1dB. It demonstrates that the motion of vortices within the row of antidots causes smaller losses than the motion in the superconducting matrix. On the one hand, this is unexpected. The motion of vortices between antidots will cause a temporary local switch to the normal state of the area between the antidots. Since the rows of antidots already represent a suppression of the current carrying cross section one would expect an enhancement of the microwave losses.[15] On the other hand, the residence time of vortices in the superconductor are shorter for guided motion than for vortices traveling in the superconducting matrix. This effect could even be enhanced by a hoppinglike motion, where the vortices rapidly jump between antidots and remain longer in the antidots. This hoppinglike motion would agree with simulations of vortex motion in arrays of antidots.[24] In this temperature regime, the impact of vortex motion on microwave losses decreases with temperature. Finally at $T < 82$ K, $\Delta S_{21} \approx 0$, i.e., vortex motion has no effect on microwave losses any more. In contrast to the situation for decreasing temperatures, the transition back to AHE dominated vortex motion with increasing temperature occurs gradually. It seems that guidance is switched off individually in the different double rows.

In conclusion, we demonstrated that a transition in the vortex motion and vortex mobility can be is induced by micropatterning of superconducting thin films. The competition between the AHE and the guidance of vortices by rows of antidots leads to a simultaneous change in the sign of the Hall voltage, the critical current density and microwave transition coefficient. Close to $T_c$ the AHE dominates and vortices shuttle between the rows, whereas at lower temperatures the vortices follow the guidance provided by the rows of antidot. Microwave measurements demonstrate the difference in vortex mobility in the different phases. The different dc and microwave experiments in combination with micropatterning of thin high-$T_c$ superconducting film might be a powerful way toward strategic manipulate vortices and its analysis that could pave the route toward interesting and innovative fluxonic effects and concepts.

The authors would like to thank H.-W. Wingens, H.P. Bochem, M. Nonn, N. Klein, and A. Offenhäuser for their valuable support. This work was supported by the ESF program "Nanoscience and Engineering in Superconductivity—NES."


[1] A. Maeda, Y. Inoue, H. Kitano, S. Savel'ev, S. Okayasu, I. Tsukada, and F. Nori, Phys. Rev. Lett. **94**, 077001 (2005).
[2] A. N. Lykov, Solid State Commun. **86**, 531 (1993).
[3] M. Baert, V. V. Metlushko, R. Jonckheere, V. V. Moshchalkov, and Y. Bruynseraede, Phys. Rev. Lett. **74**, 3269 (1995).
[4] A. M. Castellanos, R. Wördenweber, G. Ockenfuss, A. v. d. Hart, and K. Keck, Appl. Phys. Lett. **71**, 962 (1997).
[5] M. Lange, M. J. Van Bael, Y. Bruynseraede, and V. V. Moshchalkov, Phys. Rev. Lett. **90**, 197006 (2003).
[6] S. Raedts, A. V. Silhanek, M. J. Van Bael, and V. V. Moshchalkov, Phys. Rev. B **70**, 024509 (2004).
[7] R. Wördenweber, A. M. Castellanos, and P. Selders, Physica C **332**, 27 (2000).
[8] R. Wördenweber, P. Dymashevski, and V. R. Misko, Phys. Rev. B **69**, 184504 (2004).
[9] J. E. Villegas, S. Savel'ev, F. Nori, E. M. Gonzalez, J. V. Anguita, R. Garcia, and J. L. Vicent, Science **302**, 1188 (2003).
[10] J. Van de Vondel, C. C. de Souza Silva, B. Y. Zhu, M. Morelle, and V. V. Moshchalkov, Phys. Rev. Lett. **94**, 057003 (2005).
[11] C. C. de Souza Silva, A. V. Silhanek, J. Van de Vondel, W. Gillijns, V. Metlushko, B. Ilic, and V. V. Moshchalkov, Phys. Rev. Lett. **98**, 117005 (2007).
[12] B. Y. Zhu, F. Marchesoni, and F. Nori, Phys. Rev. Lett. **92**, 180602 (2004).
[13] K. K. Likharev, Sov. Phys. JETP **34**, 906 (1972).
[14] R. Wördenweber, J. S. K. Sankarraj, P. Dymashevski, and E. Hollmann, Physica C **434**, 101 (2006).
[15] A. Lukashenko, A. V. Ustinov, A. P. Zhuravel, E. Hollmann, and R. Wördenweber, J. Appl. Phys. **100**, 023913 (2006).
[16] S. J. Hagen, C. J. Lobb, R. L. Greene, M. G. Forrester, and J. H. Kang, Phys. Rev. B **41**, 11630 (1990); S. J. Hagen, A. W. Smith, M. Rajeswari, J. L. Peng, Z. Y. Li, R. L. Greene, S. N. Mao, X. X. Xi, S. Bhattacharya, Q. Li, and C. J. Lobb, *ibid.* **47**, 1064 (1993).
[17] P. Ao, J. Phys.: Condens. Matter **10**, L677 (1998).
[18] H. J. Jensen, P. Minnhagen, E. Sonin, and H. Weber, Europhys. Lett. **20**, 463 (1992).
[19] R. A. Ferrell, Phys. Rev. Lett. **68**, 2524 (1992).
[20] A. van Otterlo, M. Feigel'man, V. Geshkenbein, and G. Blatter, Phys. Rev. Lett. **75**, 3736 (1995).
[21] D. I. Khomskii and A. Freimuth, Phys. Rev. Lett. **75**, 1384 (1995).
[22] N. B. Kopnin, Phys. Rev. B **54**, 9475 (1996).
[23] J. Kolacek and P. Vasek, Physica C **336**, 199 (2000).
[24] C. Reichhardt, C. J. Olson, and F. Nori, Phys. Rev. B **58**, 6534 (1998).